Supporting Information for

Charge-Carrier Dynamics in Vapour-Deposited Films of the Organolead Halide Perovskite $CH_3NH_3PbI_{3-x}Cl_x$

C. Wehrenfennig, M. Liu, H. J. Snaith, M. B. Johnston and L. M. Herz

A. Sample Preparation

Thin films of $CH_3NH_3PbI_{3-x}Cl_x$ perovskite were deposited by dual source evaporation as described in detail in ref. 1. Lead chloride ($PbCl_2$) and methylammonium iodide (CH_3NH_3I) were deposited simultaneously onto 2 mm thick z-cut quartz substrates (for photoexcited measurements) or high-resistivity silicon (for dark measurements) under high vacuum. Before starting the evaporation, the tooling factor (which is a ratio of the material deposited on the sensors to that on the samples) was estimated for each source individually.

Approximately 500 mg of CH_3NH_3I and 100 mg of $PbCl_2$ were loaded into separate crucibles and the substrates were placed in a substrate holder above the sources. To eliminate volatile impurities in the chamber before coating the substrates with perovskite, the two crucibles were heated above the desired deposition temperatures under high vacuum (10^{-5} mbar) for approximately 5 min. To prepare representative perovskite films, key deposition parameters such as the deposition rates and duration for the two sources were set as previously optimized for best performance of the material in solar cells. [1] This includes using a CH_3NH_3I:$PbCl_2$ molar ratio of 4:1 and deposition rates of 5.3 Å s^{-1} for CH_3NH_3I (crucible temperature around 116°C) and 1 Å s^{-1} for $PbCl_2$ (crucible temperature of around 320°C), maintained for approximately 128 min of evaporation. The substrate holder was rotated to ensure uniform coating while the film was deposited on the substrate. Annealing the as-deposited films at 100°C for 45 min in a N_2-filled glove box enabled full crystallization of the perovskite, darkening the colour and resulting in an apparent growth of crystal features visible in SEM images. [1] The resulting film thickness is about 330 nm. Samples on silicon for dark THz transmittance measurements consisted of two subsequent depositions.

Figure S1 shows Scanning Electron Microscope (SEM) images of $CH_3NH_3PbI_{3-x}Cl_x$ perovskite films deposited under identical conditions on three different substrates. The top image shows the perovskite film as incorporated into a solar cell fabricated in an identical way to the best-performing device reported in Reference 1, while the middle image shows the films

resulting from direct deposition on z-cut quartz (used to extract charge carrier dynamics and mobility) and the bottom image shows film formation on silicon (used to extract the dielectric function in the THz regime). Images were taken with a Hitachi S-4300 microscope. Acceleration voltages were 3kV for the device image and 5kV for the films on quartz and Si. The emission current was 10 μA. A platinum layer of ~3nm thickness was sputtered onto the cleaved samples prior to taking the images.

Comparison of the images reveals similar film morphology and formation on the three different substrates, i.e. good homogeneity of all films with constant thickness and without pin-hole formation. This observation suggests that evaporation of the materials consistently avoids any de-wetting issues that typically dominate formation of films processed from solution.

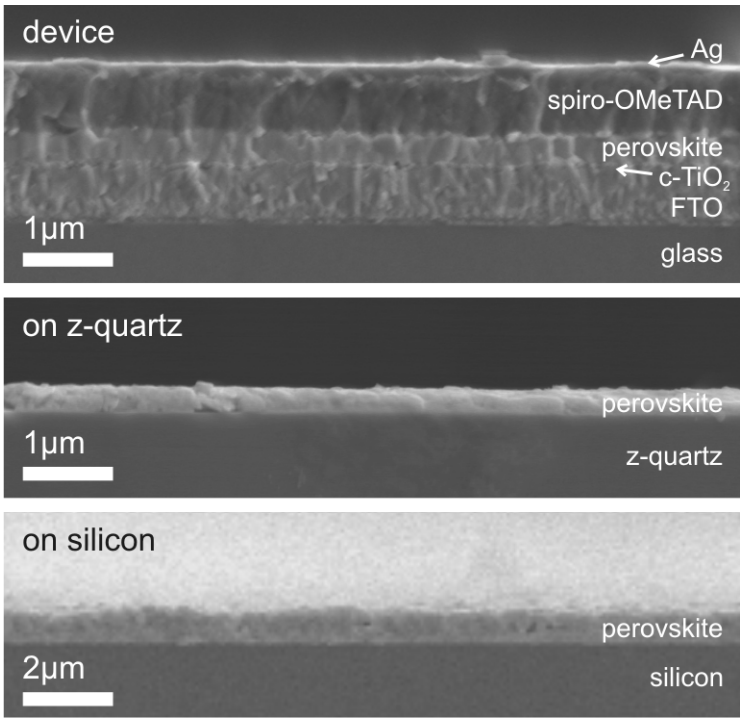

Figure S1: Cross-sectional scanning electron microscope images of evaporated films of the perovskite $CH_3NH_3PbI_{3-x}Cl_x$ deposited on different substrates under otherwise identical conditions. Top: on compact TiO_2 on FTO as part of a photovoltaic device structure. Middle: on z-cut quartz. Bottom: on silicon.

B. THz Time-Domain Spectroscopy

Our optical-pump-THz-probe setup (described in more detail previously[2]) uses a Ti:Sapphire regenerative amplifier to generate 40 fs pulses at 800 nm wavelength and a repetition rate of 1.1 kHz. Terahertz pulses are generated by optical rectification in 450 μm thick (110)-GaP and detected by electro-optic sampling in a ZnTe crystal (0.2 mm (110)-ZnTe on 3 mm (100)-ZnTe). Pulses for optical excitation of the samples at a wavelength of 550 nm have been generated using an optical parametric amplifier (OPA). Optical excitation was carried out from the non-substrate side of the film. The diameters of pump and probe beam at the sample position are 2.6 mm and 1.5 mm (FWHM). Dark spectra were acquired by measuring THz transmission of the coated against the uncoated part of a half-coated sample. Measurements have been performed with the entire THz beam path (including emitter, detector and sample) in an evacuated chamber at pressure of $< 10^{-1}$ mbar.

C. Derivation of photoconductivity and charge carrier mobility from change in THz electric field transmission

The sheet photoconductivity ΔS of a thin film between two media of refractive indices n_A and n_B, under the condition that the thickness of the film is much smaller than the THz wavelength, may be expressed as[3,4]

$$\Delta S = -\epsilon_0 c(n_A + n_B)\left(\frac{\Delta T}{T}\right), \quad (1)$$

where $\Delta T = T_{\text{illuminated}} - T$ is the photoinduced change in terahertz electric field. Here, T and $T_{\text{illuminated}}$ are the transmitted terahertz electric fields of the sample in the dark and after photoexcitation respectively. In our experiment the sample film is surrounded by vacuum from one side, hence $n_A = 1$ and in contact with the z-cut quartz substrate with THz-refractive index $n_B = 2.13$ from the other side.

In order to derive the charge-carrier mobility μ from the photoinduced sheet conductivity, the number of photo-excited charge carriers N needs to be determined using

$$N = \varphi \frac{E\lambda}{hc}(1 - R_{\text{pump}})(1 - T_{\text{pump}}) \quad (2)$$

Here, E is the energy contained in an optical excitation pulse of wavelength λ, R_{pump} is the reflectivity of the sample at normal incidence of the excitation beam, T_{pump} the (small) fraction of light transmitted through the sample and φ is the ratio of free charge carriers created per photons absorbed, commonly referred to as the photon-to-charge branching ratio, which is

technically undetermined in the experiment and related to factors such as the exciton binding energy in the material. We argue however in the main manuscript that there is some evidence making it appear likely that φ is not substantially lower than unity.

The charge carrier mobility μ is given by

$$\mu = \frac{\Delta S \, A_{\text{eff}}}{Ne} \tag{3}$$

where A_{eff} is the effective area of the overlap of optical pump and THz probe pulse taking into account the Gaussian beam profiles, and e is the elementary charge. With φ unknown, the quantity which can be directly derived from the experiment is the effective mobility $\tilde{\mu} = \varphi\mu$ where

$$\varphi\mu = -\varepsilon_0 c(n_A + n_B)\frac{A_{\text{eff}}\, hc}{E\, e\, \lambda\, (1 - R_{\text{pump}})(1 - T_{\text{pump}})}\left(\frac{\Delta T}{T}\right) \tag{4}$$

Because $0 \leq \varphi \leq 1$, the effective mobility represents a lower limit, which becomes identical to the acutal mobility for full photon to free carrier conversion. The determined charge carrier mobility arises from the contributions of both electrons and holes, which cannot be separated. Therefore the extracted mobility value is the sum of electron and hole mobilities.

To allow accurate determination of φμ we ensured that excitation conditions are in the linear regime. We have evaluated the dependence of the initial amplitude of the THz response on excitation fluence and found that nonlinear processes such as two-photon absorption only show a significant effect at fluences beyond 50 μJ cm^{-2}. Our carrier mobility calculation is based on data taken up to 32 μJ cm^{-2} and therefore not affected.

D. Fits to THz photoconductivity transients

As described in the main manuscript, the recombination dynamics of the free charge carrier density $n(t)$ may be governed by mechanisms of first, second and third order, through the following rate equation:

$$\frac{\mathrm{d}n}{\mathrm{d}t} = -k_3 n^3 - k_2 n^2 - k_1 n \,, \tag{5}$$

The experimentally observed quantity is the photoinduced THz transmission change $x(t) \stackrel{\text{def}}{=} (\Delta T/T)(t)$, which is linearly related to the free carrier density (see (1) and (3)):

$$n(t) = \varphi\, C\, x(t) \,. \tag{6}$$

Here $C = \tilde{n}_0/x(0)$ is the proportionality factor between the immediate THz response $x(0)$ and the absorbed photon density

$$\tilde{n}_0 = \frac{E\lambda\,\alpha(\lambda)}{hc\,A_{\text{eff}}}\left(1 - R_{\text{pump}}\right), \tag{7}$$

which can be calculated from the pump beam parameters and the absorption coefficient of the sample α at the excitation wavelength λ. As mentioned in the previous section, due to the onset of non-linear interactions, $x(0)$ does not remain proportional to $\tilde{n}_0$ at very high excitation fluences (> 50 μJ cm^{-2}). Therefore we determine *C* based on the initial THz response in the linear excitation regime.

Substituting (6) into (5) we obtain

$$\frac{\mathrm{d}x}{\mathrm{d}t} = -C^2\varphi^2 k_3 x^3 - C\varphi k_2 x^2 - k_1 x \tag{8}$$

$$= -A_3 x^3 - A_2 x^2 - A_1 x$$

with $A_i = C^{i-1}\varphi^{i-1}k_i$. We fit numerical solutions to this equation simultaneously to all acquired THz transients of a fluence-dependent set (i.e. there is only one globally optimized value A_i for each rate constant, which is applied to all fluences). As the photon-to-free-carrier conversion ratio φ is unknown, we can, strictly speaking, only determine the values $\varphi^2 k_3$, φk_2 and k_1 from our fits. These equal the actual decay rate constants k_3, k_2 and k_1 in case the material exhibits full photon-to-free-charge conversion.

To account for the spatially varying charge density profile, our fit routine takes into account the exponential charge density profile created by the pump beam by dividing the sample into 50 equally thick slabs and computing the decay function for all of these individually.

E. Fit of THz Permittivity Spectra

The THz permittivity spectra shown in Figure 2 of the main manuscript suggest the presence of two phonon modes in the investigated spectral range. The contribution of these modes can be modelled as Lorentzian oscillators resulting in the Drude-Lorentz response described by the equation: [5]

$$\epsilon_{\text{ph}}(\omega) = -\Delta\epsilon_s \frac{\omega_0^2}{\omega^2 - \omega_0^2 + i\,\gamma\omega} \tag{9}$$

Here, $\Delta\epsilon_s$ is the contribution of the mode to the static permittivity, ω_0 its (angular) resonance frequency and γ its half line width. The complete expression includes the sum of the two oscillator terms as well as the (high-frequency) background permittivity ϵ_∞ arising from all contributions above the accessible frequency range.

$$\epsilon(\omega) = \epsilon_{\mathrm{ph}}^{(1)}(\omega) + \epsilon_{\mathrm{ph}}^{(2)}(\omega) + \epsilon_\infty \tag{10}$$

This complex valued function was fitted simultaneously to the real and imaginary part of the measured permittivity. The results are summarized in **Table S1**. The low-frequency permittivity (i.e. the high-frequency background for the range below 0.5 THz) may be calculated as

$$\epsilon_{\mathrm{s}} = \epsilon_\infty + \Delta\epsilon_{\mathrm{s}}^{(1)} + \Delta\epsilon_{\mathrm{s}}^{(2)}. \tag{11}$$

The spectral resolution of the measurement is given by the Fourier-transform limit through the length of the acquired interval in the time-domain (Δt = 5 ps) resulting in $\Delta\omega = 2\pi/\Delta t$ = 1.26 THz. The widths of the Drude-Lorentz peaks determined through our fits (2γ > 1.26 THz) are therefore not affected by the spectral resolution limit. The phonon lifetimes can be directly obtained from these line width as $\tau = 1/\gamma$ (ref. 5).

	$\boldsymbol{\epsilon_{\mathrm{ph}}^{(1)}}$	$\boldsymbol{\epsilon_{\mathrm{ph}}^{(2)}}$	$\boldsymbol{\epsilon_\infty}$	ϵ_{s}
$\boldsymbol{\Delta\epsilon_s}$	4.8	8.0	6.8	19.6
$\boldsymbol{\omega_0 = 2\pi f_0}$ **[THz]**	6.0	12		
$\boldsymbol{\gamma}$ **[THz]**	1.6	5.1		

Table S1: Results of the fit of Equation (10) to the THz permittivity spectra. Note that ϵ_{s} is given as calculated from equation (11) and not itself a fit parameter.

References

1. M. Liu, M. B. Johnston and H. J. Snaith, *Nature,* 2013, **501**, 395-398.

2. P. Tiwana, P. Parkinson, M. B. Johnston, H. J. Snaith and L. M. Herz, *J. Phys. Chem. C,* 2010, **114**, 1365-1371.

3. H.-K. Nienhuys and V. Sundström, *Phys. Rev. B,* 2005, **71**, 235110.

4. R. Ulbricht, E. Hendry, J. Shan, T. F. Heinz and M. Bonn, *Rev. Mod. Phys.,* 2011, **83**, 543-586.

5. M. Fox, *Optical Properties of Solids,* 2nd ed., Oxford University Press, 2010.